Influence of Heat Inputs on Weld Profiles and Mechanical Properties of Carbon and Stainless Steel

L. O. Osoba*, W. A. Ayoola, Q. A. Adegbuji, O. A. Ajibade

Department of Metallurgical and Materials Engineering, University of Lagos, Lagos State, Nigeria.

ABSTRACT: This study examines the effect of heat input on the weld bead profile, microstructure and mechanical properties of single V- joint welded carbon and stainless-steel plates. The as-received sample steel plates were sectioned into eight pieces; dimension 75 X 30 X 10 mm thicknesses. Shielded metal arc welding (SMAW) of heat inputs 1250 and 2030 J/mm was used to produce full penetration bead on the plates. Although visual inspection indicated that some of the welds were macro defect free, austenitic stainless steel exhibited more weld distortions than the carbon steel and this was partially attributed to its lower carbon content and the width to depth aspect ratio of the weld profile aside the magnitude of the induced stress. For the carbon steel, as the heat input increased, the hardness value of both the heat affected zone and fusion zone increased. In contrast, for stainless steel, the hardness values were reasonably comparable within same weld region (HAZ or FZ) irrespective of heat input. Furthermore, the ultimate tensile strength of the stainless steel decreased as heat input increased while the ductility increased with an increase in heat input, in contrast to carbon steel, where both ductility and ultimate tensile strength generally decreased.

KEYWORDS: Carbon steel, stainless steel, heat input, weld profile, heat affected zone.

[Received June 18, 2020; Revised Feb. 19, 2021; Accepted May 12, 2021] Print ISSN: 0189-9546 | Online ISSN: 2437-2110

I. INTRODUCTION

Metal alloys comprising of iron (Fe) and carbon (C) also known as steel have found applications in building construction, infrastructure such as bridge, tools, equipment, machinery, ship, vehicle components and weaponry. This ferrous based metal exhibit unique properties including, strength and good weldability depending on its composition and can be classify based on its carbon content (ASM Int, 2018). Mild steel and or low carbon steel, wherein, the main alloying element carbon is between the ranges of 0.05 – 0.25% usually have good formability, low strength and good weldability. Medium carbon steel, with carbon content that ranges from 0.25 to 0.70% is known with good ductility, strength, ease of machining and good wear resistance and find applications for large forging parts and in automobile parts. High carbon steel has a carbon range between 0.6 % and 1.50 % and manganese content of between 0.30 to 0.90 % (Regan, 2010). Increasing carbon content being the primary alloying element, for improved hardness and strength of steels is often the most economical means to improve the service performance. However, damaging effects of higher carbon content include reduced ductility, impaired weldabilty and impact toughness. In the Heat Affected Zone of weldment, materials with high carbon content greater than 0.50 % are known for high hardness with consequent brittle joint, aside the significant increases in susceptibility to weld cracking (Agarwal et al. 2019).

Traditionally, welding involves the use of a heat source to generate a high temperature region that melts the material, such that upon solidification, the joints are fused together (Mohammed et al., 2017). There are different types of welding processes, among which are Gas Welding, Arc Welding, Friction Welding and Laser Welding. It is a generally known fact that process parameter such as Welding Current, Arc Voltage and Welding Speed play significant roles in determining the Weld Profile and Magnitude of Heat Input delivered into joints during welding and the subsequent performance of the welded joint (Moi et al., 2019). Therefore, in the current study, the effect of weld heat input on mechanical properties such as hardness, tensile strength and weld profile is evaluated.

Ali and Mohammed (2018) studied the mechanical properties of the welded joints of low carbon steel welded using two different welding process (Arc welding and gas welding) with three different edge type and specific coupon size of two groups having dimension 200 and 100 mm in length with square cross-section area of 10 x 10 mm. The effect of heat inputs on mechanical properties such as, impact, tensile, bending and hardness were studied. Results obtained shows that Arc-welding is better than Gas-welding because the latter method leads to a reduction in mechanical properties. Shen *et al*. (2012) studied the effect of welding parameters on weld bead geometry and HAZ. Their finding indicated that welding parameters and flux basicity greatly affected the depth of penetration of the weld bead. Arul, *et al.* (2016) carried out experiments using modified refractory flux

*Corresponding author: losoba@unilag.edu.ng

doi: http://dx.doi.org/10.4314/njtd.v18i2.8

welding and studied the effects of welding variables on formation of root welds, including the deposit inside the groove and deposit outside the groove also called root bead and root reinforcement, respectively. This study also showed that welding variable produced a profound and sometimes conflicting effect on the root weld's shape. As an instance, the deposition rate and the depth of joint penetration increases as the current increased. In contrast, slag pocket was noticed and root bead shape deteriorated, which may engender joint failure.

Talabi *et al.* (2014), studied the effect of welding variables on the mechanical properties of welded carbon steel plate, welded using the shielded metal arc welding (SMAW) method. Welding current, arc voltage, welding speed were the investigated welding parameters. The welded samples were sectioned and machined to standard configurations for hardness, tensile, and impact toughness tests. Results showed that selected welding parameters had pronounce effects on the mechanical properties of the samples welded. Increases in the welding current and arc voltage led to a decrease in yield strength, tensile strength and impact toughness but increased the hardness.

Although prior reduction in tensile and yield strengths was noticed, it increased thereafter as the welding speed increased. This behaviour is associated with the fact that increased voltage and current necessitated increased heat input, which could create room for defect formation, as such, the observed reduced mechanical properties. Bodude, et al. (2015), and a group of authors Fathi et al.,(2019), studied the effect of heat input on the mechanical properties of low carbon steel using two welding processes, namely, Shielded Metal Arc Welding (SMAW) and Oxy-acetylene Welding (OAW) as well as the effect of welding type on the mechanical properties of welding joints. Two different edge preparations on a specific size, 10 mm thick low-carbon steel, with the different welding parameters and different mild steel electrode gauges were evaluated. The tensile strength, impact strength and hardness of the welded joint were appraised. While the impact strength of the weldment increased with the increase in heat input, the tensile strength and hardness reduced with the increase in heat input of the weld. It was also observed that straight edge preparation had a poorer mechanical property as compared with V-grooved edge preparation under the same conditions. Microstructural examinations of the weldment revealed that the cooling effect of different quenching media has significant effect on the resulting microstructure of the weldment. Both ferrite and pearlite were noticed in the resulting microstructure, but the proportion of pearlite to ferrite varied under different conditions.

Jatti, et al. (2014) studied the effect of welding current, welding voltage and welding speed on tensile strength, micro-hardness and microstructure of austenitic 202 grade stainless steel weldment produced by shielded metal arc welding (SMAW) by varying the heat input. Cr-Mn SS and 308L SS was material used in the investigation while solid electrode was used as the filler material. Result showed that tensile strength decreased with increase in heat input as evidence in scanning electron microscopy of tensile test fractured surfaces that exhibited ductile and brittle failure features. Micro hardness test values indicated that hardness of weld material increases with increase in heat input in the Fusion Zone and decreases in the Heat Affected Zone. Light optical microstructural evaluation reveal presence of small size dendrite with short inter-dendritic line spacing in the fusion zone of the low heat input welds. While bigger size dendrites with longer inter-dendritic line spacing were observed in the fusion zone of the joint welded at high heat input. Furthermore, as the heat input increases, it was observed in the HAZ that the amount of grain coarsening increased.

Wan Muda, et al. (2015) studied the effect of welding heat input on the distribution of microstructure formation and its mechanical properties at coarse grain heat affected zone (CGHAZ) of the ABS Grade A steel. Three heat input combinations designated as high heat (2.25 kJ/mm), medium heat (1.22 kJ/mm) and low heat (0.99 kJ/mm) were used to weld the specimen using shielded metal arc welding (SMAW) process. The microstructure formation at CGHAZ was consisting of Widmannstetter ferrite (WF), grain boundary ferrite (GBF) and pearlite (P). Significant grain coarsening was observed at the CGHAZ of all the joints, and it was found that the extent of grain coarsening at CGHAZ also increased along with the heat input. The results of the mechanical investigation indicated that the joints made by using low heat input exhibited higher hardness and impact toughness value than those welded with medium and high heat input. It was concluded that higher heat input can cause the expansion towards the microstructure's grain size but also will lead to lower hardness and affect the toughness value. In the current study the effect of weld parameters on mechanical properties and weld profile of high carbon steel and stainless steel is investigated. Significant influence of heat input on weld profile of welded carbon and stainless steel are compared using constant heat input.

II. MATERIALS AND METHODS

A. Materials

The materials of interest used in this study include low carbon steel plates, 316 austenitic stainless-steel plates, 6 mm E7018 electrodes and 6 mm ARCALOY 308l-15 electrodes, which were used for the 316 austenitic stainless steel (ASS). In preparing the weldment for macro/micro examination, standard metallographic procedure was used. The low carbon steel plate and stainless steel plates and their respective nominal chemical composition were obtained from Dormanlong Engineering Limited, Idi-Oro, Lagos State, Nigeria where the welding process was carried out.

B. Sample preparation

The as-received carbon and stainless-steel plates are of 10 mm thickness each and was sectioned into eight pieces each using cutting machine with each having a length of 75 mm and breadth of 30 mm. A milling machine was used to prepare the edges at 30^° on the long side. The sample was arranged to make a single-V joint with a consistent 3 mm root gap between the plates before welding the samples using SMAW process with different welding parameters.

C. Welding Procedure

In order to investigate the effect of heat input on the weld profile and mechanical property of low carbon steel and 316 stainless steels, SMAW process was used for welding the samples using the welding parameters presented in Table 1. In this study, other welding parameters such welding speed, arc length, torch angle, electrode diameter were kept constant to study the effect of welding current and voltage. The welding procedures were carried out at Dormalong Engineering Ltd and standard Welding Inspection Procedure (WIP) was followed. Eq. (1) was used for the calculation of the heat input (Amuda et al., 2020).

$$\text{Heat input (HI)} = \frac{\text{current(A) x voltage(V)}0.06}{travel\ speed(s)} \quad (1)$$

where: Heat Input (kJ/mm), Arc voltage (volts) and Travel speed (mm/min)

Table 1: Welding parameters.

Parameter	Welding current (A)	Voltage (V)	Welding speed (mm/min)	Heat input (kJ/mm)
1	80	26	100	1.25
2	130	26	100	2.03

D. Microstructural Investigation

The microstructures of the metal substrate were observed with the aid of an optical microscope CETI 0703552 at the Metallography Laboratory of the University of Lagos. The images obtained were recorded as datum microstructures in order to compare the variation after thermal cycling. The substrate surfaces were ground, polished and etched before the microstructural examination. Plane grinding was carried out with silicon carbide grit paper (600 to 1200 micron) to avoid creating artificial porosity by fracturing the particles. In order to obtain a good final surface finish, a 1 µm colloidal silica paper was used to obtain a good contrast. Aqua reagent, a commonly used solution for making visible the microstructure of non-ferrous metals was used as the etchant in the investigation. This was followed by metallographic examination of the mirror-like polished surfaces under the optical microscope.

E. Micro Hardness Testing

The hardness test was carried out at the Metallurgy Laboratory of Department of Metallurgical and Materials Engineering, University of Lagos in accordance with ASTM E384 standards for Vickers hardness of materials using a MMT-X7A micro hardness tester HV5. An average of 4 indentations was carried out at every zone considered for a period of 10 seconds under a load of 980.66 mN.

III. RESULTS AND DISCUSSION

A. Analysis of Chemical Composition of the Carbon Steel and Stainless Steel Material

Table 2 shows the result of the chemical analysis of the as-received carbon steel and stainless steel materials used in this study. The table gives the details of principal elements such as carbon (C), silicon (Si), manganese (Mn), vanadium (V) and chromium (Cr) with varying composition present in the steels. These elements are known to have significant influence on the mechanical properties and microstructural transformation that occur in welded carbon steels and stainless steels. For example, formation of refined grain structure has been attributed to the presence of Mn and V while the formation of carbides is attributed to the presence of carbon (Keehan, 2004).

Table 2: Chemical composition of the as-received carbon steel and stainless-steel material.

Elemental composition (wt. %)	Material Types	
	Carbon steel	Stainless steel
C	0.123	0.0166
Si	0.342	0.477
Mn	1.39	0.882
P	0.0068	0.04
S	-	0.0033
Cr	0.0248	16.63
Ni	0.0265	10.21
Mo	0.0047	2.08
V	-	0.083
Fe	97.8	69.62

B. Influence of Heat Input on the Weld Bead Profile of Welds

Figure 1 and 2 shows the weld bead profiles of the carbon steel and ASS weldment produced at different heat input. The macrographs revealed that increases in the heat input caused significant change in the HAZ profile.

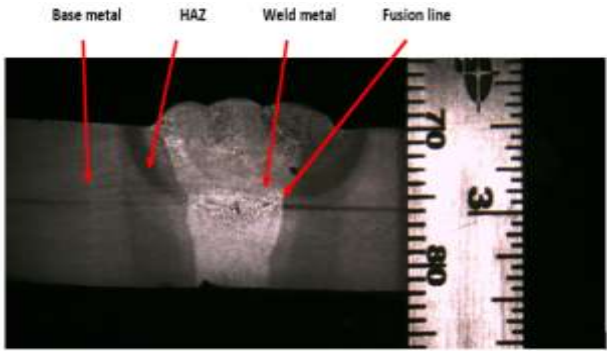

Figure 1: Macroprofile of carbon steel welded at heat input of 2030 J/mm.

More noticeable from the macrographs is that the HAZ becomes wider as the magnitude of heat input increases. Although, this observation is less pronounced with stainless

steel, as shown in Figures 3 and 4, however the stainless are more distorted relative to the carbon steel.

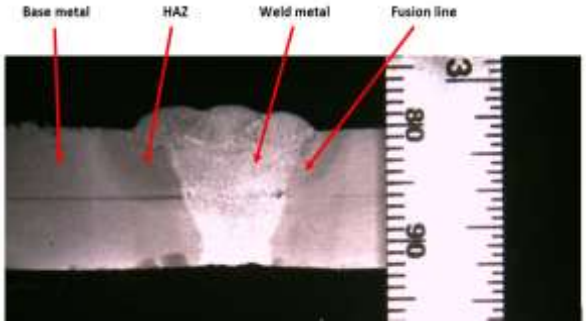

Figure 2: Macroprofile of carbon steel welded at heat input of 1250 J/mm.

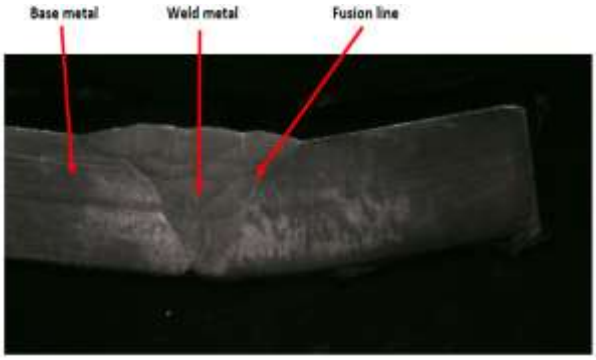

Figure 3: Macroprofile of stainless steel welded at heat input of 2030 J/mm.

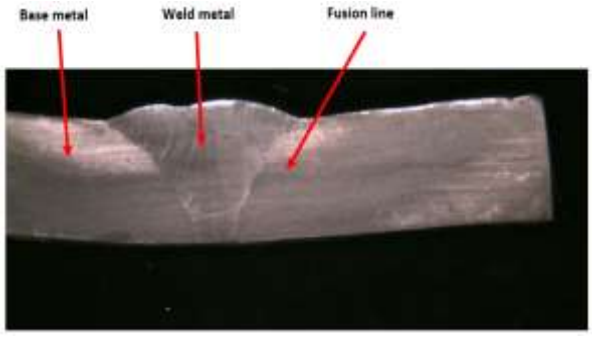

Figure 4: Macroprofile of stainless steel welded at heat input of 1250 J/mm,

C. Aspect Ratio (Top Width to Depth Ratio)

Measurements of the top weld width to depth of penetration were carried out with the aid of AxioVision SE64 Rel. 4.9.1 software. Figures 5-8 shows the measurements of the depth and width. The effect of heat input on the top width to depth ratio (aspect ratio), known as a measure of weldment to cracking or cracking index (Osoba et. al. 2012) was measured and presented in Table 3 and Figure 9. For the carbon steel, the top width to depth ratio for the high heat input (2030 J/mm) is 1.911 while that for the low heat input (1250 J/mm) is 1.926.

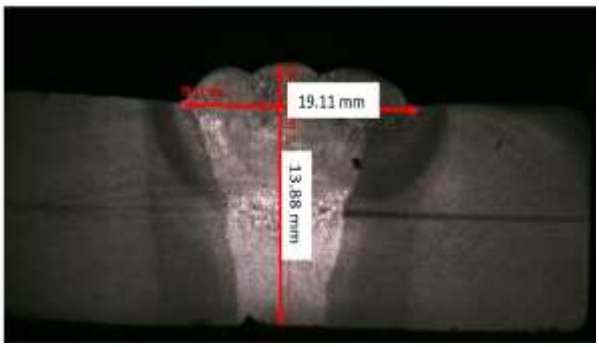

Figure 5: Macroprofile of carbon steel welded at heat input of 2030 J/mm.

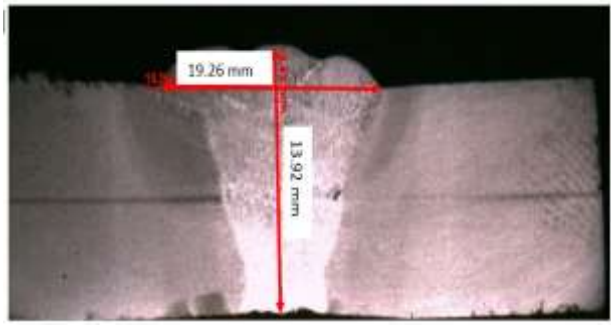

Figure 6: Macroprofile of carbon steel welded at heat input of 1250 J/mm.

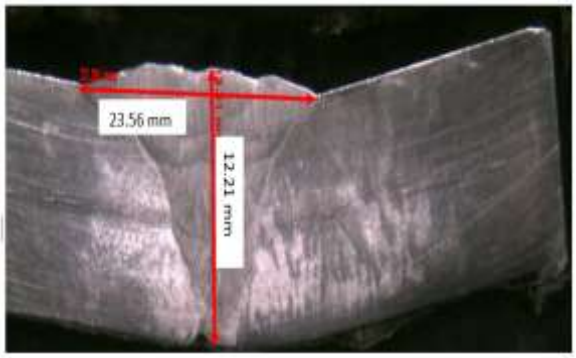

Figure 7: Macroprofile of stainless steel welded at heat input of 2030 J/mm.

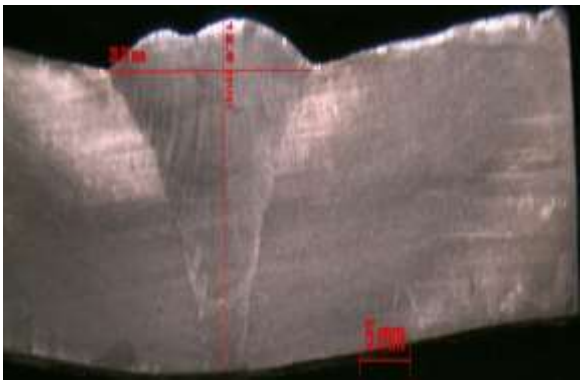

Figure 8: Macroprofile of stainless steel welded at heat input of 1250J/mm.

The top width to depth ratio for stainless steel weldment with a heat input of 2030J/mm is 2.356, while the ASS weldment with a heat input of 1250J/mm produced a top width to depth ratio of 2.029. There was full penetration across all the welded samples, which could be attributable to the heat input applied. However, as the heat input increased, the top width of the weld bead increased, an indication of the significant effect of heat input. The aspect ratio increased with increase in heat input for the stainless-steel welded samples, whereas, the carbon shows no differences, as shown in Figures 7 and 8 respectively. The significance of the top width to depth ratio results is the indication that the stainless steel is far more susceptible to microcracks relatives to the carbon steel weldment, which may not be unconnected with significant amount of distortions in the stainless steel weldment.

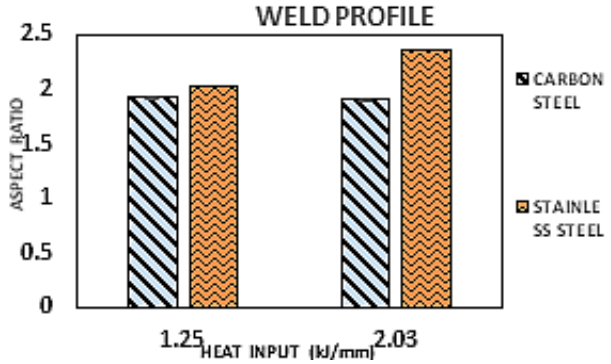

Figure 9: Effect of Heat Input on top Width to Depth ratio.

Table 3: Cracking index against Heat input.

Material	Heat input (kJ/mm)	Aspect ratio
Carbon Steel	2.03	1.911
	1.25	1.926
Stainless Steel	2.03	2.356
	1.25	2.029

D. As Received Microstructure and Influence of Welding Current on the Weldment Microstructure

The optical microstructures of the as-received low carbon steel and the ASS are shown in Figures 10 (a) and (b). The as-received microstructure of the low carbon steel clearly showed ferrite matrix and the distribution of pearlite while that of the stainless steel shows ferrite-ferrite grain boundaries with dispersed precipitates of carbide. However, the microstructure of the weldment shows that the microstructures were distorted during the welding process such that the applied energy (heat input) re-distributes the phase orientation.

Figures 11 and 12 reveal the heat affected zone (HAZ) and the fusion zone (FZ) of the low carbon steel welds produced with 1050 and 2030 J/mm. Microstructural evaluation of the low carbon steel weldment produced could be used to evaluate the effect of welding current on the

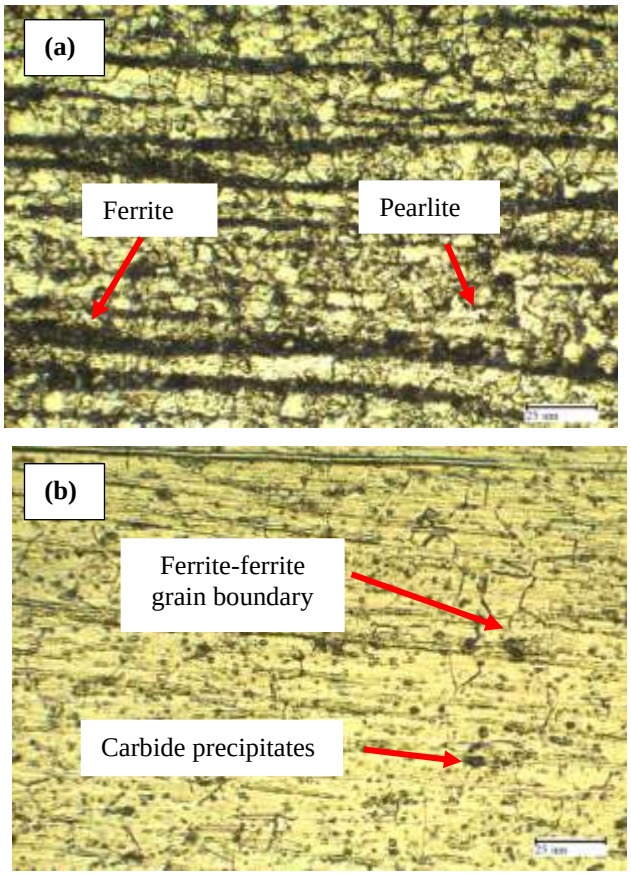

Figure 10: (a) Optical micrograph of the as-received low carbon steel (b) Optical micrograph of the as-received SS stainless steel.

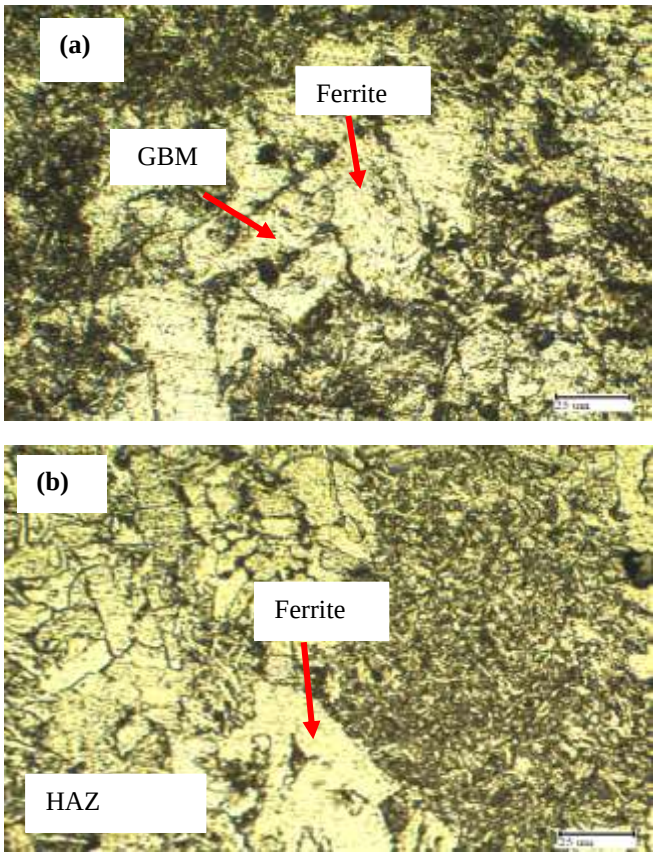

Figure 11: Optical micrograph of low carbon steel weld produced with current of 80A (a) Fusion zone (b) Heat affected zone.

microstructural inhomogeneity of the weldment. In welding of steels, there are different solidification paths and transformation sequences and most of the steel weld begins solidification with the formation of δ-ferrite and in most cases, accompanied by the nucleation of austenite on the δ-δ-ferrite grain boundaries (Keehan, 2004). In Figure 13 microstructural features such as coarse ferrite grains were also observed in the weld HAZ. This suggests that at high welding current, the cooling rate was slow with transformation of austenite (γ) to α-ferrite (Sindo Kou, 2003).

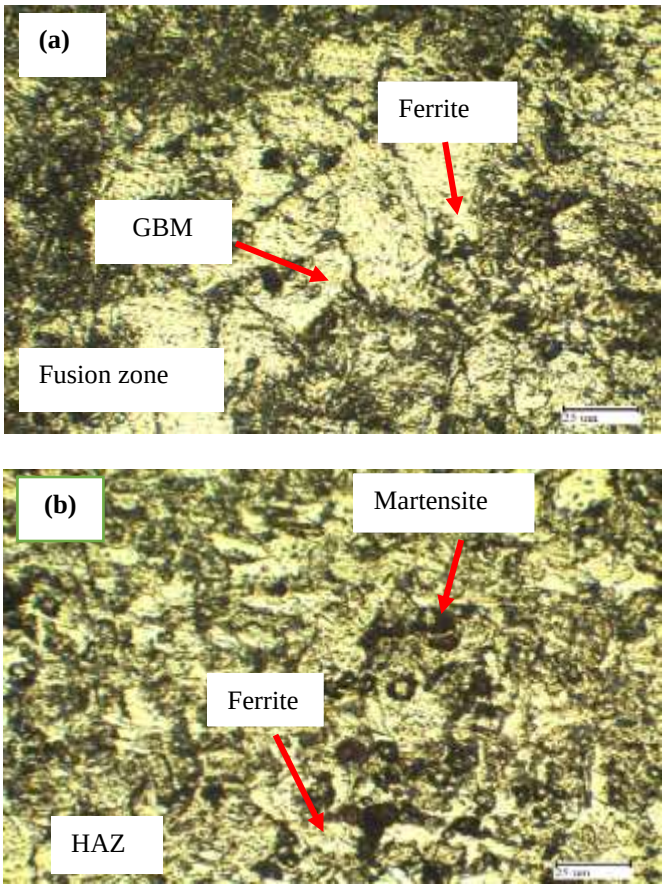

Figure 12: Optical micrograph of low carbon steel weld produced with current of 130A (a) Fusion zone (b) Heat affected zone.

In Figure 12, microstructural features indicating grain boundary maternsite were observed in the fusion zone while ferrite, martensite and some carbide precipitates were observed in the HAZ of the weld produced with current of 130 A. The formation of these martensites in the HAZ of the weldments indicated rapid cooling during the weld silidification (Kou, 2003; Nhung et al., 2017).

E. Influence of welding current on the microstructure of SS stainless steel weldments

The influence of welding current on the microstructure of SS stainless steel is shown in Figures 13 and 14. In Figure 13, the weld was produced using a current of 80 A and heat input of 1.25 kJ/mm. The microstructure depicts the predominance of columnar grains in the fusion zone while δ-ferrite, grain boundary martensite and few carbide precipitate were observed at the weld HAZ. This grain boundary martensite is suspected to be responsible for the high hardness values observed in the weld HAZ from the micro hardness test result.

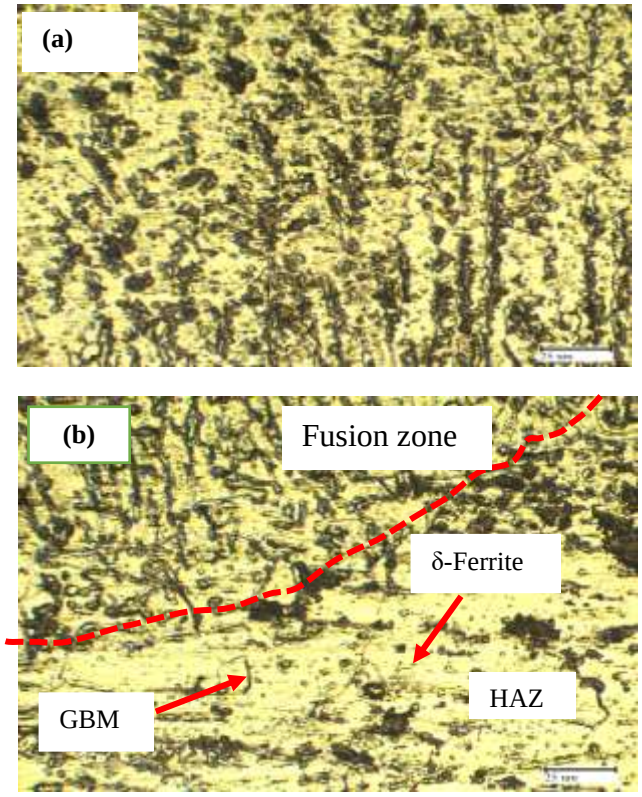

Figure 13: Optical micrograph of SS weld produced with 80A current (a) Fusion zone (b) Heat affected zone.

E. Influence of Welding Current on the Microstructure of SS Stainless Steel Weldments

The influence of welding current on the microstructure of SS stainless steel is shown in Figures 13 and 14. In Figure 13, the weld was produced using a current of 80 A and heat input of 1.25 kJ/mm. The microstructure depicts the predominance of columnar grains in the fusion zone while δ-ferrite, grain boundary martensite and few carbide precipitate were observed at the weld HAZ. This grain boundary martensite is suspected to be responsible for the high hardness values observed in the weld HAZ from the micro hardness test result.

Figure 14 is the micrograph of the SS stainless steel produced with a high current (130A) and heat input of 2.03 kJ /mm. The micrograph shows the presence of equiaxed grains in the weld fusion zone while inter-dendritic martensite coarse grain ferrite as well as grain boundary martensite were observed in the HAZ of the weld. The presence of this coarse grain ferrite suggest that the cooling rate was slower in part of the HAZ when compared to the weldment produced with low current (80A) and heat input of 1.25 kJ/mm this could be detrimental to the material strength as it results to microstructural inhomogeneity.

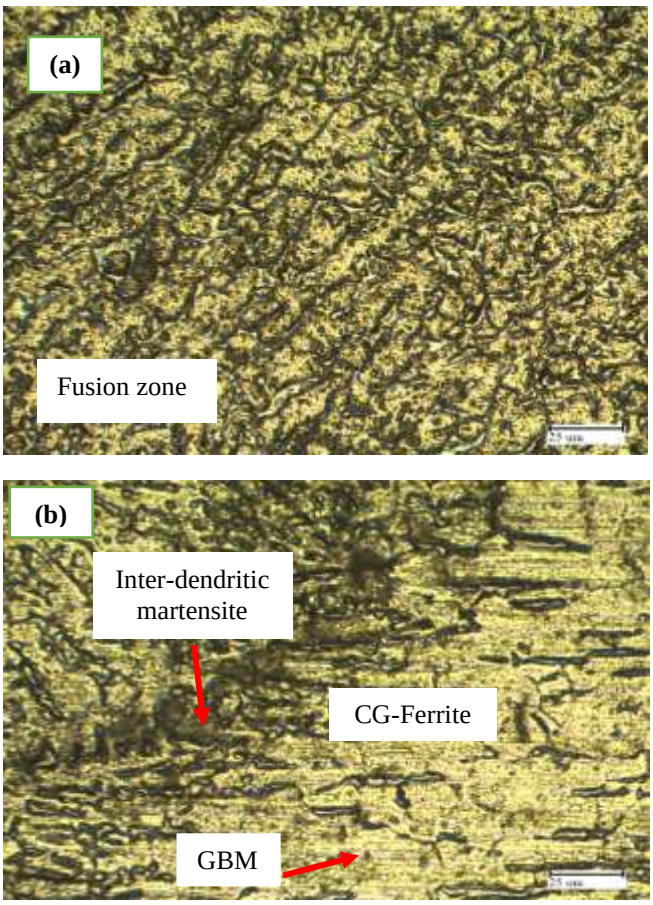

Figure 14: Optical micrograph of SS stainless steel weld produced with high current 130A (a) Fusion zone (b) Heat affected zone.

F. Hardness Test

The Vickers hardness values of the weld zone of the welded samples at different heat input are presented in Table 4.

Table 4: Hardness value of the control samples.

Material	Hardness values (HV)			
	Control	Heat input (kJ/mm)	Weld zone	
			HAZ	Fusion
Carbon steel	283.00 ± 1.2	1.25	220.60±10.4	215.05 ± 3.3
		2.03	269.00 ± 8.2	317.60 ± 4.0
Stainless steel	332.95 ± 5.8	1.25	309.45 ± 2.5	288.25 ± 6.5
		2.03	290.00±16.8	279.65 ± 8.5

The hardness values in the HAZ and the FZ of the welded low carbon steel increased with an increase in heat input. This observation can be attributed to the formation of a martensite phase and/or the precipitation of carbides as shown in the micrographs in Figures 11 and 12, and consistent with previously reported investigation by Ali and Mohammed (2018). The hardness values in the HAZ and the FZ of the welded stainless steel shows that the hardness of the HAZ and FZ are reasonably comparable within same weld region (HAZ or FZ) irrespective of the heat input. The higher the heat input the slower the cooling rate which allows for grain refinement within the HAZ and leads to the formation of coarse grains (Jovicic et al., 2015; Gu et al. 2019; Amuda et al. 2020) that should engender relatively softer HAZ.

It was observed that the hardness of the fusion zone slightly increased as the heat input increased from 1250 to 2030 J/mm which may not be unconnected to the increased formation of an inter-dendritic martensitic phase in the fusion zone (Figure 14b). Comparing the hardness behavior of the carbon steel and stainless steel, it can be observed that within the HAZ region, stainless steel hardness is more than carbon steel irrespective of heat Input. Generally, the HAZ experience the least heat, such that there is no melting but microstructural modification, the extent of which depends on the alloying contents which are more in the Stainless steel compared to the carbon steel.

The FZ on the other hand experience complete melting and solidification such that cooling rate within the welds is not at equilibrium and varies significantly as the heat input varies. As observed for low heat input, the FZ hardness of the SS is higher than in CS mainly because the cooling rate in the FZ for SS is expectedly slower than CS owing to the alloying elements aside the effect of the induced stresses which cause obvious distortions of the stainless steel weldment. In contrast, at higher heat input, slower cooling in the CS welds that allows massive transformation to martensitic structure that enhances its hardness compare to the SS where the stress induced distortions were huge and may have contributed to reliving the induced stress and consequent strength.

G. Analysis of Weld Tensile Strength

The tensile behavior of welded Carbon steel samples and the unwelded base material is presented in Figure 15 and Table 5. The Figure shows that the elastic yield strength of the welded samples increases marginally, irrespective of the heat inputs, and are higher than that of the base material.

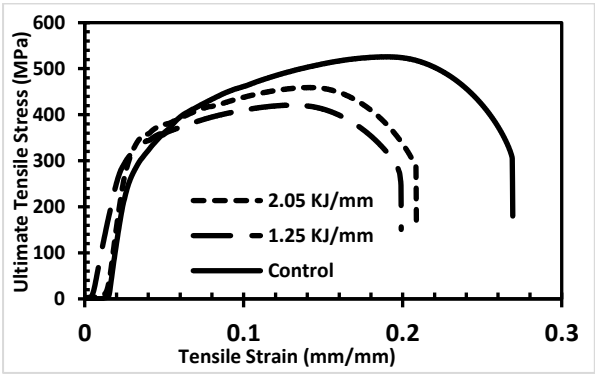

Figure 15: Welded and unwelded stress-strain curve for carbon steel.

Table 5: Effect of heat input on tensile properties of carbon steel weldment.

Heat Input (kJ/mm)	Yield Strength (MPa)	UTS (MPa)	Elongation (%)
As Received (Control)	287	526	27
1.25	330	493	19
2.03	340	510	20

However, the ductility and tensile strength (UTS) of the welded samples degraded considerably compared to the base material. It is well known that welded sections in material are often sites of stress concentration for incipient cracks with consequent impairment of tensile properties. Table 6 and Figure 16 show the tensile test results of the SS welds. From the graphs, both the yield strength and ductility of the welded samples are significantly higher than that of the base material. The Ultimate Tensile Strength (UTS) of the welded SS samples are however lower than that of the base materials.

In comparison, the tensile properties of the ASS welds are generally higher as such better than the tensile properties of the CS irrespective of the heat inputs. The observed tensile behavior can be attributable to the previously discussed explanation for the hardness behavior in terms of the alloying content variations in the two materials coupled with the influence of heat input on the cooling behavior of the weld region. The results are in agreement with previously reported investigations (Talabi et al., 2014; Owolabi et al., 2016) where welded stainless steel samples gains ductility at the expense of strength as the heat input increases.

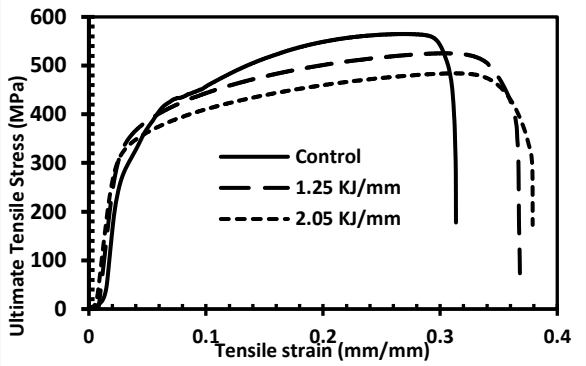

Figure 16: Welded and unwelded stress-strain curve stainless steel.

IV. CONCLUSION

The influence of heat input on the weld bead profile, hardness, tensile and microstructure of CS and SS at constant heat inputs has been investigated with the following conclusion drawn.

Heat input has a significant effect on the hardness of the heat affected zone and fusion zone of welded samples for both low carbon and stainless steel. For carbon steel, as the heat input increases the hardness value of both the heat affected zone and fusion zone increases. However, in stainless steel welds, the hardness values are essentially comparable within the heat affected zones or the fusion zone irrespective of the heat input.

The tensile properties of the stainless steel welds are generally higher or better than the tensile properties of the carbon steel irrespective of the heat inputs and this can be attributable to alloying content variations in the two materials couple with the influence of heat input on the cooling behaviour of the weld region.

ACKNOWLEDGEMENT

The authors are grateful to Dormanlong Engineering Limited, Idi-Oro, Lagos State, Nigeria for the provision of SMAW equipment and allocation of a certified welder.

REFRENCES

Ali, A. M. and Mohammed, K. A. K. (2018). Dynamic response to welded joints of low carbon steel with different edges. International Journal of Engineering Research and Technology, 11(12): 2159–2166.

Amuda, M.O.H.; L.O. Osoba; N.N. Etuk; T.F. Lawal and A.O. Adetayo. (2020). Tracking local brittle zone in the heat affected zone of girth-welded API 5L X46 pipe. Nigerian Journal of Technology (NIJOTECH), 39(2): 403-416.

Agarwal, G.; A. Kumar; I. M. Richardson and M.J.M. Hermans. (2019). Evaluation of solidification cracking susceptibility during laser welding in advanced high strength automotive steels. Materials and Design, 183: 108104.

Arul, M.M.A.; B.S.R. Sundara; R. Rajeshkumar and R. Kumar. (2016). Factors influencing submerged arc welding on stainless steel - a review. ARPN Journal of Engineering and Applied Sciences, 11(2): 1237–1241.

Fathi, M.S.A.; Q. Ismael and K.A. Saleh. (2019). An effect of welding type on the mechanical properties of welding joints. International Journal of Mechanical and Production Engineering Research and Development, 9(4): 699-707.

Gu, Y.; F. Xiao; Y. Zhou; J. Li; C. Xu and X. Zhou. (2019). Behaviors of embrittlement and softening and softening in heat affected zone of high strength X90 pipeline steels. Soldagem & Inspecao, 24:e2415.

Gupta, S. R. and Arora, N. (1991). Influence of flux basicity on weld bead geometry and heat affected zone in submerged arc welding. Indian Welding Journal, 24: 127–133.

Jovicic, R.; R. Prokic-Cvetkovic; B. Zrilic and K. Jovicic-Bubalo. (2015). Heat input welding. Zavarivanje Zavarene Konstrukcije, 60(2): 61–69. https://doi.org/10.5937/zzk1502061j

Keehan, E. (2004). Effect of microstructure on mechanical properties of high strength steel weld metals. PhD Thesis Published, Department of Experimental Physics, Chalmers University of Technology and Goteborg University, Sweden. https://doi.org/10.17863/CAM.14213

ASM International. Metals Handbook Desk Edition. (2018). In Metals Handbook Desk Edition. https://doi.org/10.31399/asm.hb.mhde2.9781627081993

Mohammed, G. R.; M. Ishak; S.N. Aqida and H.A. Abdulhadi. (2017). Effects of heat input on microstructure, corrosion and mechanical characteristics of welded austenitic and duplex stainless steels: A review. Metals, 7(39): 1-18. https://doi.org/10.3390/met7020039

Moi, S. C.; P.K. Pal; A. Bandyopadhyay and R. Rudrapati. (2019). Effect of heat input on the mechanical and metallurgical characteristics of TIG welded joints. Journal of Mechanical Engineering, 16(2): 29–40.

Nhung, L.T.; P.M. Khanh; L.M. Hai and N.D. Nam. (2017). The relationship between continuous cooling rate and microstructure on the Heat Affected Zone (HAZ) of the dissimilar weld between carbon steel and austenistic stainless steel. Acta Metallurgical Slovaca, 23(4): 363-370.

Osoba, L.O. and Ojo, O.A. (2012). Influence of laser welding heat input on HAZ cracking in newly developed Haynes 282 superalloy. Material Science and Technology. Institute of Materials, Mineral, and Mining, 28(4): 431- 436.

Owolabi, O.B.; S.C. Aduloju C.S. Metu C.E. Chukwunyelu E.C. Okwuegu. (2016). Evaluation of the effects of welding current on mechanical properties of welded joints between mild steel and low carbon steel. American Journal of Metallurgical and Materials Engineering, 1(1): 1-4.

Scott, F. R. (1998). Key Concepts in Welding Engineering–Post Weld Heat Treatment. Welding Innovation, XV(15(2)): 1-2.
http://www.jflf.org/v/vspfiles/assets/pdf/keyconcepts4.pdf

Shen, S.; I.N.A. Oguocha and S. Yannacopoulos. (2012). Effect of heat input on weld bead geometry of submerged arc welded ASTM A709 Grade 50 steel joints. Journal of Materials Processing Technology, 212(1): 286-294.

Sindo, K. (2002). Welding Metallurgy Second Edition Welding Metallurgy. Wiley Online Books, John Wiley & Sons, Inc. Available online at: Online ISBN:9780471434023/|DOI:10.1002/0471434027. Accessed on April 12, 2020

Wan Muda, W. S. H.; N.S. Mohd Nasir; S. Mamat and S. Jamian. (2015). Effect of welding heat input on microstructure and mechanical properties at coarse grain heat affected zone of ABS grade a steel. ARPN Journal of Engineering and Applied Sciences, 10(20): 9487–9495.